JOURNAL OF WATER AND LAND DEVELOPMENT
e-ISSN 2083-4535

Polish Academy of Sciences (PAN) Institute of Technology and Life Sciences – National Research Institute (ITP – PIB)

JOURNAL OF WATER AND LAND DEVELOPMENT
DOI: 10.24425/jwld.2021.139025
2021, No. 51 (X–XII): 152–162

Forest cover change detection in relation to climate variability and LULC changes using GIS and RS techniques. A case of the Kafa zone, southwest Ethiopia

Dejene Beyene Lemma ✉, Kinde Teshome Gebretsadik, Seifu Kebede Debela

Jimma Institute of Technology, Faculty of Civil and Environmental Engineering, Jimma University, Jimma, P.O.Box: 378, Ethiopia

RECEIVED 24.08.2020 REVIEWED 19.02.2021 ACCEPTED 05.07.2021

Abstract: Ethiopia has lost sizable forest resources due to rapid population growth and subsequent increase in the demand for agricultural land and fuel woods. In this study, GIS and remote sensing techniques were used to detect forest cover changes in relation to climate variability in the Kafa zone, southwest Ethiopia. Landsat Thematic Mapper (TM) images of 1986 and 1990, Enhanced Thematic Mapper plus (ETM+) image of 2010 and Landsat-8 Operational Land Imager (OLI-8) image of 2018 were acquired at a resolution of 30 m to investigate spatial-temporal forest cover and land use changes. A supervised image classification was made using a maximum likelihood method in ERDAS imagine V9.2 to identify the various land use and land cover classes. Both spectral (normalised difference vegetation index – *NDVI*) and post classification change detection methods were used to determine the forest cover changes. To examine the extent and rate of forest cover changes, post classification comparisons were made using ArcGIS V 10.4.1. A net forest cover change of 1168.65 ha (12%) was detected during the study period from 1986 to 2018. The drop in the *NDVI* from 0.06–0.64 in 1986 to (–0.08)–0.12 in 2018 indicated a marked forest cover change in the study area. The correlation of *NDVI* values with climate data indicated the forest was not in a stable condition. The declining of the forest cover was most likely caused by climate variability in the study area.

Keywords: change detection, climate variability, forest cover change, GIS, Kafa zone, land use and land cover (LULC), remote sensing

INTRODUCTION

About 30% of global land surface is covered with forests which are the most important providers of ecosystem services and human wellbeing [Kipkemboi *et al.* 2019; Zawadzki *et al.* 2005]. Forests also play an important role in climate change regulation and carbon sequestration [Negassa *et al.* 2020]. Ethiopia's forest resources have been seriously depleted as a result of rapid population growth and subsequent rising demand for farm and grazing land and fuel woods [Ayele *et al.* 2019]. Although data are limited, about 35–40% of Ethiopia's landmass was covered by high forests just before the turn of the 19th century [Cheng *et al.* 1998; Othow *et al.* 2017]. The country lost much of its natural forests before the turn of 20th century [Oljirra 2019; Tadesse *et al.* 2014]. Nearly 2.8 mln ha of natural forests disappeared between 1990 and 2010, which translates into an annual loss of 1.4 mln ha [Negassa *et al.* 2020]. Unprecedented changes occurred to the forest cover as a result of the pressure from economic development [Attri *et al.* 2015] Unsustainable consumption of forests and forest products also resulted in the degradation of forest resources of Ethiopia [Engdawork, Bork 2014]. The lack of a sustainable forest management policy also contributed to high deforestation rates in Ethiopia [Danano *et al.* 2018]. Around 95% of Ethiopia's remaining natural forests are located in the southwest region [Tadesse *et al.* 2014]. Deforestation has significant impacts, including extensive soil erosion, loss of biodiversity, water quality degradation, forest product loss, drought and flooding and low agricultural productivity [Attri

et al. 2015; Tadesse *et al.* 2014]. It also contributes to enhanced greenhouse effects by the decreasing of the carbon stock in forest biomass [Gebru 2016].

Various efforts have been made to conserve the unique natural forest of the Kafa zone. One such effort is the establishment of Biosphere Reserves (BR) as a forest management strategy to integrate resource conservation and sustainability [Ferreira *et al.* 2020; Austrian MAB Committee 2011]. BR seems very crucial for countries like Ethiopia, where a large proportion of the population depend on natural resources. This is why Ethiopia has already dedicated five of its important biodiversity areas (Lake Tana and Kafa, Sheka, Yayu and Majang forests) to biosphere reserves [Austrian MAB Committee 2011]. The designation of BR is based on appropriate zoning of different resource use and participatory governance to promote conservation, sustainable development, logistic support to research and environmental education, and the contribution to climate change mitigation and adaptation [Ferreira *et al.* 2020].

Land use and land cover change (LULCC), the modification of the Earth's surface as a results of human activity, becomes recognised as the main driving force behind unprecedented changes to forest cover and environmental processes [Alqurashi, Kumar 2014; Hassan *et al.* 2016].

Several studies indicate that a number of efforts have been made to map, monitor, identify and model LULCC at the local, regional and global scales [Maina *et al.* 2020]. Remote sensing (RS) and geographic information system (GIS) are the fundamental methods to quantify, map and detect LULCC for advanced ecosystem management [Fichera *et al.* 2012; Weng 2001] because of their accurate geo-referencing procedures, suitability for computer processing and repetitive data acquisition [Hassan *et al.* 2016]. Also GIS and RS methods provide a significant potential to analyse urban and pre-urban environment with a higher degree of accuracy and precision [Appiah *et al.* 2015].

Landsat data have been commonly used in the RS for quantification, mapping and detection of LULCC because of their accurate geo-referencing procedures, digital format suitable for computer processing and repetitive data acquisition [Hassan *et al.* 2016; Lu *et al.* 2016]. RS data provide detail, accurate, cost effective and up-to-date information in data-poor regions where up-to-date and reliable spatial information is scarce [Dong *et al.* 1997]. Advancement in digital image processing offers unprecedented opportunities to detect LULCC more accurately over increasingly large areas with minimum costs and shortest possible time [Attri *et al.* 2015; Coppin *et al.* 2004]. The temporal resolution at which remotely sensed images are acquired is also suitable for the monitoring of land cover changes [Caldeira 2012; Othow *et al.* 2017; Pongratz, Yismaw 2014]. The LULCC study using RS and GIS methods provide credible policy recommendations to manage natural resources and monitor environmental changes [Alawamy *et al.* 2020; Wang *et al.* 2020].

A lot of techniques have been devised to detect attributable earth surface changes [Hassan *et al.* 2016; Zhu, Woodcock 2014]. Change detection uses multi-temporal datasets to identify differences in the status of earth attributes by observing them at different dates [Gandhi *et al.* 2015; Singh 1989]. The digital change detection process has been used to determine LULCC based on multi-temporal remotely sensed data [Coppin *et al.* 2004; Kennedy *et al.* 2009]. Numerous change detection techniques, such as image differencing, post-classification comparison (PCC), vegetation index differencing (*VID*) and principle components analysis (PCA), have been used to monitor LULCC using remotely sensed data [Hassan *et al.* 2016; Lu *et al.* 2016]. Of these, PCC is the most widely used procedure as it minimises errors associated with multi-temporal images recorded under different conditions [Ziboon *et al.* 2013]. PCC compares classifications of images independently produced at different dates without any adjustment needed [Al-Doski *et al.* 2013; Hassan *et al.* 2016]. On the other hand, the normalised difference vegetation index (*NDVI*) employs the multi-spectral remote sensing data technique to find the vegetation index with few electromagnetic spectrum band combinations [Coppin *et al.* 2004; Gandhi *et al.* 2015]. The *NDVI* is based on the threshold values (e.g., 0.1, 0.15, 0.2, 0.25, 0.3, 0.35, 0.4 and 0.6) [Gandhi *et al.* 2015; Negassa *et al.* 2020]. Satellite images must be processed prior to the actual change detection to establish direct link between remote sensed data and biophysical Earth attributes [Coppin, Bauer 1996]. No study has been conducted to integrate geo-information tools with RS data and techniques to detect forest cover changes in the study area. The lack of reliable data to monitor the extent and pattern of forest cover change, high deforestation rate and significant impacts of deforestation on local, regional and global climates were the main reasons to conduct the study.

MATERIALS AND METHODS

DESCRIPTION OF THE STUDY AREA

The study was conducted in the Kafa Biosphere Reserve (KBR) in South Nation, Nationalities and Peoples Regional State, in the Kafa zone (Fig. 1). The Kafa Biosphere Reserve is situated in Southwest Ethiopia (latitude: from 35°29'50.55" to 36°47'33.78" N; longitude: from 35°48'50.57" to 35°44'34.30" E). The aim of a Biosphere Reserve is to manage resources in an integrated manner through resource conservation, planning and sustainable uses by dividing into three areas or zones [Ferreira *et al.* 2020]. The total area of the KBR, including candidate core zones (currently it lacks statutory conservation status) is 760,144 ha. The KBR harbours 41,319 ha of core zones, 161,427 ha of buffer zones and 337,885 ha of transition zones [NABU 2017]. The southern boundary of the KBR follows partly the Bonga National Forest Priority Area (NFPA), whilst the eastern boundary follows the Adiyo district. The Gojeb River and Gewata-Yeba NFPA forms the northern boundary of the KBR [Bender, Tekle 2019]. The area contains more than 50% of the remaining Ethiopian mountain forests and genetically diverse wild *Coffea arabica* [NABU 2017]. The area receives average annual rainfall of 1500 mm at lowlands and 2000 mm at the high elevations. Agriculture is the dominant economic activity of the Kafa zone. Other sectors, such as services, tourism, trade and manufacturing, are strongly dependent on the backward and forward linkages of agricultural activities [NABU 2017].

DATA COLLECTION

Combination of GIS and RS techniques were used to detect spatial-temporal forest cover change in the Kafa zone. Field visits were made to collect primary data, identify various land use land

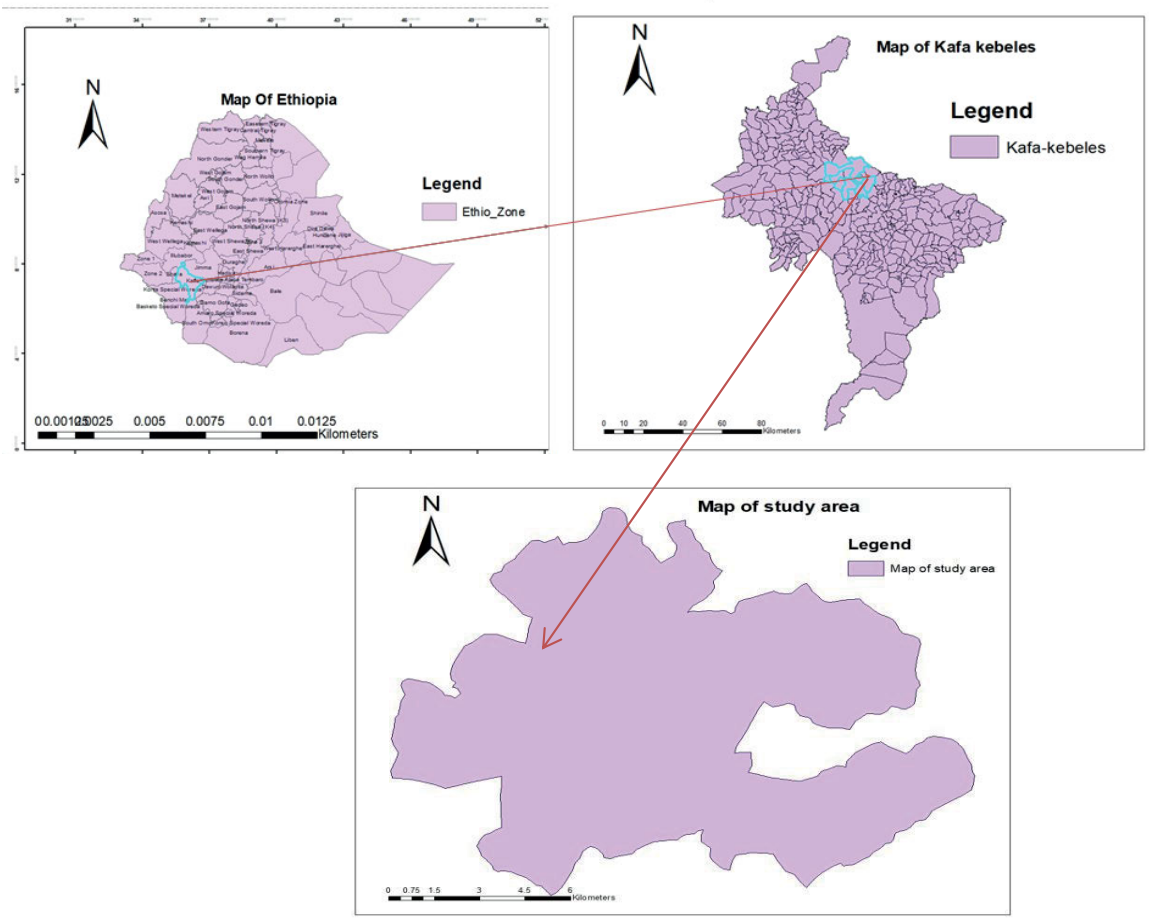

Fig. 1. Map of the study area; source: own elaboration

cover types and forest cover features, and to take GPS readings for all the land-cover boundaries. The data were used for the final image classification, sampling sites verification and the validation of the land use land cover map. Cloud free remotely sensed satellite images (Landsat 7 TM of 1986 and 1990, Landsat 7 ETM+ of 2010 and Landsat 8 OLI of 2016 and 2018) were downloaded from the United States Geological survey site (https://earthexplorer.usgs.gov/) at spatial resolution of 30 × 30 m for the study area. An area equals to the KBR (5406.31 km^2) was delineated and sliced out from the full scene of four year satellites images. For the climate variability study, temperature and rainfall data were obtained from the national meteorological agency. Data were also collected from the Kafa Zone Department of Forest and Environmental Protection and other stakeholders. The various land-cover types were identified through satellite image manipulation and by observing the available land cover types. Photographs were taken from the four land use and land cover areas using a digital camera for mapping and quantify forest cover change. ERDAS and ArcGIS v 10.4.1 were used throughout the forest cover change detection analysis. Bonga and the surrounding areas were selected as the study site due to easy access, metrological data limitations and high deforestation and settlement rates.

DATA PROCESSING AND ANALYSIS

Remote sensing data were used to detect forest cover and other land cover changes in the Kafa zone from 1986 to 2018. Landsat TM images of 1986 and 1990, Landsat ETM$^+$ image of 2010 and Landsat 8 OLI images of 2018 were rectified, geometrically corrected and geo-referenced to the Universal Transverse Mercator (UTM) WGS 1984 [Gandhi *et al.* 2015; Negassa *et al.* 2020]. Supervised classification was employed on the Earth Resource Data Analysis System (ERDAS) IMAGINE version 9.2 and ArcGIS 10.4.1 to classify land use land cover using the decision rule of a maximum likelihood classifier algorithm. The various land cover classes and ground control points recorded during fieldwork were used as representative signatures for the various land cover types identified in the study area. Post image classification comparison change detection procedure was used to examine area and rate of forest cover changes. Four aspects of forest cover change detection characteristics were identified, such as detecting the changes, identifying the nature of changes, measuring temporal and area changes and assessing the spatial pattern of the change.

The analysis of a linear regression trend was carried out using ArcGIS V10.4.1 to simulate trends in each grid [Stow *et al.* 2007]. ArcGIS was used to reflect vegetation cover characteristics in different years of the study period. It was also used to get the relative *NDVI* value change in every pixel point as in Equation (1):

$$\theta = \frac{n\sum_{i=1}^{n} iNDVIi - \sum_{i=1}^{n} i \sum_{i=1}^{n} NDVIi}{n\sum_{i=1}^{n} i^2 - \left(\sum_{i=1}^{n} i\right)^2} \quad (1)$$

where: i is annual number; n is monitoring period (cumulative number of years), *NDVI* is mean *NDVI* value of the i^{th} year; θ is

each pixel *NDVI* trend of slope (if $\theta > 0$ then the pixel *NDVI* value in *n* years is increasing otherwise decreasing).

The pixel *NDVI* values were categorised into significant increase, slight increase, essentially the same, slightly reduced and a significant reduction to obtain statistics for vegetation changes and percentage of each class of land cover area for the study period (1986–2018). In order to remove a scan line error from the image of ETM+, pixel values of the neighbouring stripe were replaced by average pixel values in addition to the elaboration of the scan line error correction algorithm in GIS spatial tools.

CHANGE DETECTION FOR THE POST IMAGE CLASSIFICATION

In the post classification change detection method, the 1986, 1990, 2010 and 2018 land use land cover classified images were reclassified with ArcGIS 10.4.1 and ERDAS 9.2. The area of changes was extracted through a direct comparison of the individual classified imagery and the comparison was based on statistical data derived from each individual image. In addition, a land use land cover change detection matrix was generated to examine trends and pattern of land use land cover change of the area, specifically for the forest cover change detection. The rate of forest cover change was computed as in Equation (2):

$$r = \frac{Q_2 - Q_1}{t} \tag{2}$$

where: r is rate of forest cover change, Q_2 is recent year forest covers (ha), Q_1 is initial year forest cover (ha) and t is time interval between initial and recent years. From the land use land cover map images, the 1986, 1990, 2010 and 2018 forest cover map of the study area were generated.

SPECTRAL CHANGE DETECTION

There are a large number of techniques in the spectral change identification category [Xiuwan 2002]. Spectral change detection techniques rely on the principle that land cover changes result in persistent changes in the spectral signature of the affected land surface. Spectral change detection methods are numerical indicators which use the visible and near infrared electromagnetic spectrum for the analysis of remotely sensed satellite images to assess the presence or absence of green vegetation [Verbesselt *et al.* 2012]. The *NDVI* is the most common and widely used index for the forest cover change detection [Huete *et al.* 2002]. The *NDVI* process needs to separate each and every band to find vegetation cover in a multi spectral satellite image. The *NDVI* value depends on the absorption of red light by plant chlorophyll and the reflection of infrared radiation by water-filled leaf cells to identify the level of vegetation in an area [Gandhi *et al.* 2015]. The *NDVI* value is calculated from reflectance measurements in the red and near infrared (*NIR*) portion of the electromagnetic spectrum [Negassa *et al.* 2020]. It takes the (*NIR–RED*) difference and normalised to balance out the effects of uneven illumination, such as shadows of clouds or hills [Gandhi *et al.* 2015]. The empirical *NDVI* (red *NDVI – RNDVI* and green *NDVI – GNDVI*) values can be computed as in Equations (3) and (4).

$$RNDVI = \frac{NIR - RED}{NIR + RED} \tag{3}$$

$$GNDVI = \frac{NIR - GREEN}{NIR + GREEN} \tag{4}$$

where: *RED* is visible red reflectance (band wavelength range of 600–700 nm) and *NIR* is near infrared reflectance (band wavelength range 750–1300 nm). GREEN is electromagnetic spectrum (band wavelength of 550 nm).

The vegetation condition can be explained by *NDVI* values which range between –1 and +1. Very low *NDVI* values (≤0.1) correspond to a barren area (no vegetation cover); moderate *NDVI* values (0.2–0.3) represent shrub and grassland areas, while green healthy high vegetation cover areas, e.g. rainforests have *NDVI* values of 0.6–0.8. The *NDVI* value close to 0 represents bare soil, while negative *NDVI* values correspond to water bodies [Mancino *et al.* 2014]. In this study, the *NDVI* analysis was conducted using Arc GIS 10.4.1 which automatically computed the maximum, minimum, mean and standard deviation *NDVI* values for the forest cover change trend analysis.

RELATING SPECTRAL CHANGE WITH CLIMATE VARIABILITY

There is a close relationship between geographic features and related degree of mutual geographical elements. Average monthly temperature and precipitation data are processed from four metrological stations (Bonga, Wushwush, Shebe and Chida) located very close to the study area. Most of the data available encompass the entire time span of the study period, with the exception of a new monthly record. Missing data were artificially extrapolated using data available from the neighbouring station. *NDVI* values were correlated with year to year average annual temperature and precipitation using the pixel spatial correlation. Correlation coefficients were used to reflect the sequence of climate variability and degree of the *NDVI* correlation. The range of correlation coefficient varies from –1 to 1 and the graphical representation shows the relation of annual temperature and precipitation with the *NDVI* value.

RESULTS AND DISCUSSIONS

LAND USE LAND COVER CLASSIFICATION (1986–2018)

Image classification is the process of sorting pixels into a finite number of individual classes based on their data file values. If a pixel satisfies certain set of criteria, it is assigned to the class that corresponds to those criteria. In this study, land use land cover was classified as settlement, farm land, forest cover and wetland. The land use land cover classification of 1986, 1990, 2010 and 2018 are shown in Figure 2. In this study, land use land cover was classified as settlement, farm land, forest cover and wetland. All data sets of 1986 image, reflect forest and farmland cover larger areas; settlement covers smaller areas while wetland covers minimal areas. The middle region has quite a large area of settlement.

The LULC classification based on1986 and 1990 images indicate that the difference was insignificant. There was resettlement in different kebele (smallest administrative unit) in

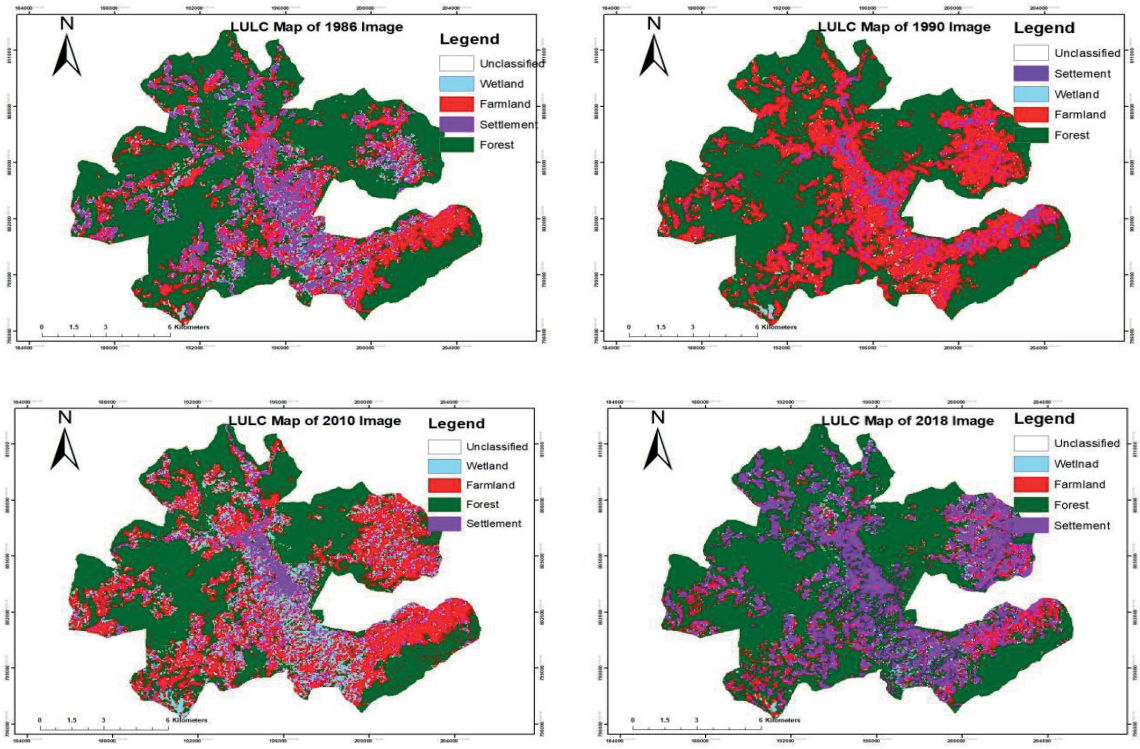

Fig. 2. Land use and land cover (LULC) classification image of 1986, 1990, 2010 and 2018; source: own study

1990. The resulting settlement area was quite smaller compared to that of 1986. In 1990, forest occupied larger areas and it was followed by farmland. The supervised image classification of 2010, forest and farmland occupied the largest area while settlement and wetland the smallest area. In the LULC classification of 2010 image, settlement disturbs the forest cover areas (green colour). In the same manner, in 2018, forest covers most areas whereas settlement and wetland occupied the remaining area.

LAND USE LAND COVER CHANGE MAPPING IN 1986–2010

The major land cover changes observed during the study period occurred due to the reduction in both forest and wetland areas. A considerable increase in the overall area of settlement and farmland has been observed. LULC change between 1986 and 2010 was computed using ArcGIS, ERDAS and Microsoft Excel and presented as a matrix (Tab. 1, Fig. 2).

LAND USE LAND COVER CHANGE MAPPING IN 2010–2018

Major changes detected during this period show that there was a decrease in the overall area of forest cover, with the net change of –322.2 ha. Additionally, the overall area of farmland and wetland decreased with the net change of –138.42 ha and –353.7 ha respectively. Settlement area increased by 814.32 ha. The overall land use land cover change detected in 2010–2018 is shown in Table 2 and Figure 3.

Table 1. Land use and land cover (LULC) change confusion matrix of 1986–2010

Year	2010						
1986	LULC type	wetland	farmland	forest	settlement	grand total	loss
	wetland	255.15	537.57	471.87	315.27	1 579.86	1 324.7
	farmland	271.89	1 803.69	642.42	775.62	3 493.62	1 689.9
	settlement	332.64	792.90	314.19	637.56	2 077.29	1 439.7
	forest	366.75	1 192.86	7 723.20	715.32	9 998.10	2 274.9
	summary	10 419.57					
	grand total	1 226.43	4 327.02	9 151.70	2 443.77	17 148.87	
	gain	971.28	2 523.33	1 428.50	1 806.21		
	net change	–353.43	833.40	–846.50	366.48		
	net persist	–1.38519	0.462053	–0.11	0.574816		

Source: own study.

Table 2. Land use and land cover (LULC) change confusion matrix of 2010–2018

Year	2018						
2010	LULC type	wetland	farmland	forest	settlement	grand total	loss
	wetland	127.80	334.53	290.25	473.40	1 225.98	1 098.18
	farmland	398.79	2 141.10	462.51	1 322.73	4 325.13	2 184.03
	forest	168.57	886.50	7 739.37	348.75	9 143.19	1 403.82
	settlement	177.12	824.58	328.86	1 112.31	2 442.87	1 330.56
	summary	11 120.58					
	grand total	872.28	4 186.71	8 820.99	3 257.19	17 137.17	
	gain	744.48	2 045.61	1 081.62	2 144.88		
	net change	–353.70	–138.42	–322.20	814.32		
	net persist	–2.76761	–0.06465	–0.04163	0.73209807		

Source: own study.

THE NET LAND USE LAND COVER CHANGES DETECTED IN THE STUDY AREA IN 1986–2018

Data sources from the preceding sections were used to detect the net land use land cover changes in Kafa zone. The net land use land cover changes detected are shown in Table 3 and Figure 3. The area of farmland was 3496.23, 5881.5, 4325.13 and 4193.91 ha in 1986, 1990, 2010 and 2018 respectively. The farmland area increased during the period of 1986–1990. It decreased in 2010 but only a little change was observed in 2018. During the first period of 1986 to 2010, the net farmland increased to 833.4 ha but between 2010 and 2018 it was reduced to 138.42 ha. The area of farmland increased proportionally at rate of 696.96 ha during the study period between 1986 and 2018. Besides the increasing trend, farmland was converted to other land cover types.

The total land area under wetland was the smallest among land cover types in the study area. It was about 1580.76, 1225.98 and 873 ha in 1986, 2010 and 2018, respectively. The net change from 1986 to 2010 shows that the area of wetland was reduced by 353.43 ha. Between 2010 and 2018, a value similar to the one in the period between 1986 and 2010 was detected. During the period between 1986 and 2018, the net change decreased to 707.13. This might be due to the fact that most wetland area was converted to other land cover types.

The settlement area was 2077.83, 2442.87 and 3260.16 ha in 1986, 2010 and 2018, respectively. The settlement area was increased by 365.04 ha between 1986 and 2010. It was increased by 814.32 ha between 2010 and 2018. The main focus of this study was to detect the spatial and temporal distribution, historical pattern, past and current deforestation process of natural forest in the Kafa zone. Different data types and sources were integrated using different methodological approaches and various application tools to describe the magnitude of forest cover change, as well as to obtain a tangible picture of past and present forest covers in the study area. This was based on maps as well as quantitative and qualitative statistical responses.

The land use land cover change matrix shows that the pattern of forest cover area decreased from 9998.1 ha to 9151.7 ha from 1986 to 2010. It further reduced to 8820.99 ha during the period between 2010 and 2018. This indicates that net forest cover change has been declined by 846.45 ha and 322.2 ha in the intervals between 1986 and 2010 and 2010 and 2018 respectively.

Table 3. Land use and land cover change confusion matrix of 1986–2018

Year	2018						
1986	LULC type	wetland	farmland	settlement	forest	grand total	loss
	wetland	151.11	423.27	476.10	529.29	1 579.77	1 428.66
	farmland	243.36	1 679.13	976.86	595.17	3 494.52	1 815.39
	settlement	145.35	557.10	998.55	376.47	2 077.47	1 078.92
	forest	332.82	1 531.98	808.02	7 337.70	10 010.52	2 672.82
	summary	10 166.49					
	grand total	872.64	4 191.48	3 259.53	8 838.63	17 162.28	10 166.49
	gain	721.53	2 512.35	2 260.98	1 500.93		
	net change	–707.13	696.96	1 182.06	–1 171.89		
	net persist	–4.67957	0.415072	1.183776476	–0.15971		

Source: own study.

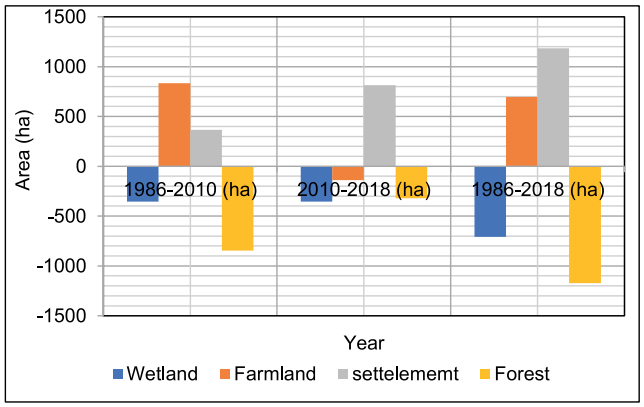

Fig. 3. Net land use land-cover change (1986–2018); source: own study

Area of forest cover was reduced by 1171.89 ha in the study area between 1986 and 2018. This might be due to the fact that the forest cover might be converted to other land cover types.

THE ANALYSIS OF RAINFALL AND TEMPERATURE TRENDS OVER THE STUDY PERIOD

Year-to-year average figures were used to filter out irregular fluctuations between successive rainfall observations and to draw average annual rainfall trend lines (Fig. 4). Thereafter, meteorological data were subjected to a linear regression analysis to show trends, intercepts, slopes and regression lines of rainfall data. Although relative variability shows an increasing trend (–0.0344 mm), absolute variability experienced a positive trend in the Bonga sub-station.

The period of 1986–1995 experienced a rapid fluctuation in annual rainfall after which rainfall went up in 1996 to reach the highest absolute variability recorded over that period. From 1996 to 2002, it showed frequent fluctuation whereas from 2003 to 2008, a relatively similar variability of annual rainfall was detected. The highest annual rainfall was recorded in 2010 and 2011. However, it exhibited frequent ups and downs within the study period and this trend picked up in 2014 (Fig. 5). The rainfall showed much volatility implying that the study area received an annual rainfall of 0.0323 mm. This had an implication for other components of weather and climate. The fluctuation had an adverse impact on the study area and neighbouring areas.

Maximum temperature and temperature trends in study area

In the time series analysis procedure adopted for this study, a simple linear regression model was applied to the corresponding times series. As shown in Figure 6, there was a statistically significant positive trend in the annual average temperature. The time series slope estimate of 0.0236°C per year was observed over the period (1986–2015).

The overall trend shows that the maximum average temperature showed a positive trend unlike minimum temperature and rainfall. This indicated an increase in air temperature. During the period of 1986–2015, the highest average maximum temperature of 29.10°C was recorded in 2008 at Bonga station and the maximum value reaches up to 38.50°C. During this period it can be seen that there was great temperature difference in 1987–1993. In 1986–1993, the maximum temperature was stable and remained below 32°C, but this value increased to 34°C

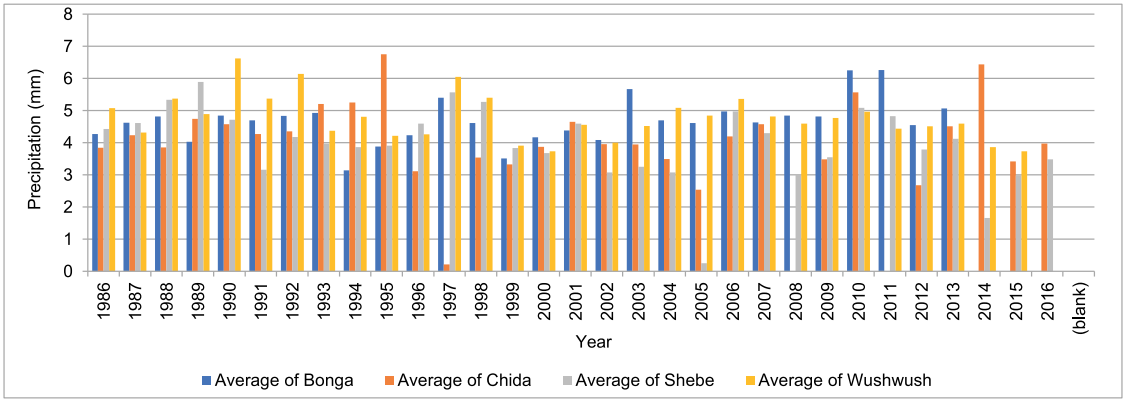

Fig. 4. Average annual rainfall data of four stations (1986–2016); source: own study

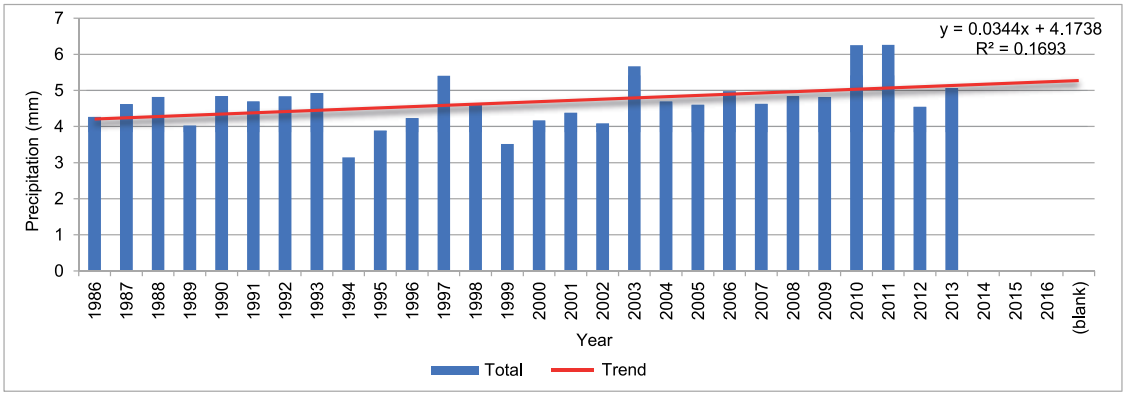

Fig. 5. Annual rainfall trend in Bonga station from 1986 to 2013; source: own study

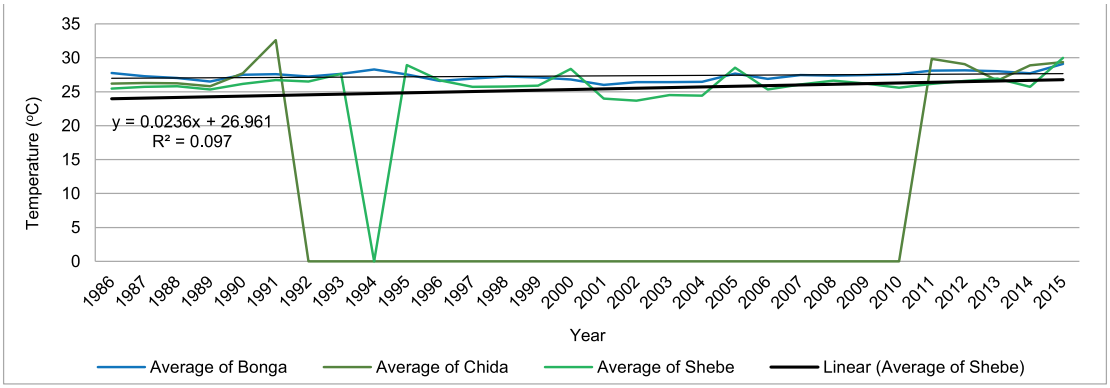

Fig. 6. Annual maximum average temperature at three stations in 1986–2015; source: own study

in 1993. In 1994–2006, the maximum temperature was relatively good, but in 2008, the highest maximum temperature of 38°C was recorded. Unfortunately, the value decreased to 31.90°C in 2009, which might be due to the beginning of the afforestation programme in 2010. Temperature trend was up and down throughout the period (1986–2015).

Minimum temperature and temperature trends in the study area

The trend of monthly average minimum temperature over the study period was obtained using linear regression best-fit lines. The annual average of monthly minimum temperatures experienced a decreasing trend with an annual decrease of 0.0079°C (Fig. 7). The trend was linear with $y = -0.0079x + 12.128$, which indicated that, in the study area and neighbouring stations, the annual average minimum temperature declined by 0.0079°C between 1986 and 2015. From 1986 to 2010, there was an incremental trend that was basically related to land use land cover change.

The annual minimum temperature recorded at the Shebe station was 9.03°C and 8.95°C in 2000 and 2002, respectively. Based on annual minimum temperature, the analysis of the Bonga station showed that the temperature in the study area was not stable in those three decades. In 1986–1996, the temperature decreased annually by –0.2315, but from 1997 to 2005, there was an increase in temperature by 0.143°C. However, in 2005–2009, there was a decrease by 0.4689°C.

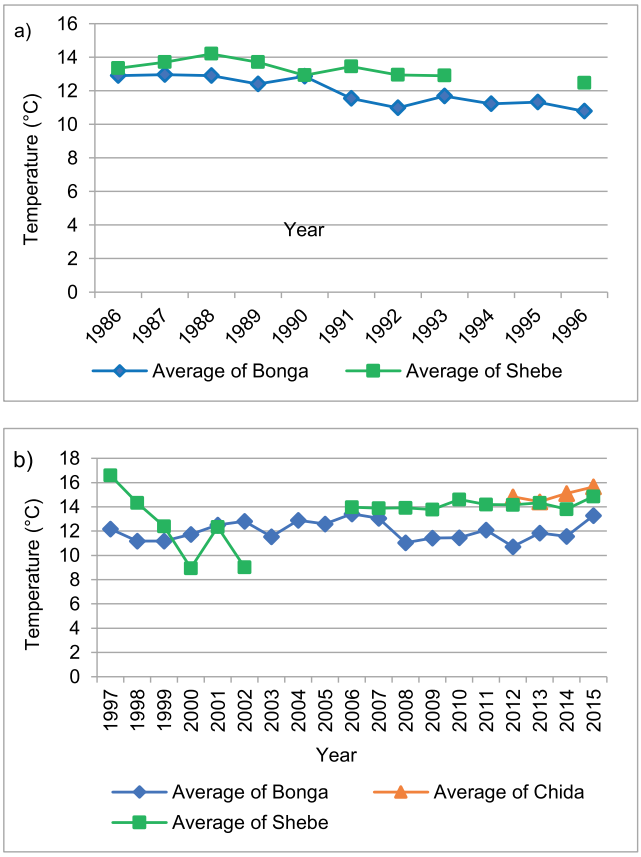

Fig. 7. Annual minimum temperature of: a) Bonga and Shebe (1986–1996), b) Bonga, Chida and Shebe stations (1997–2015); source: own study

NORMALISED DIFFERENCE VEGETATION INDEX (*NDVI*) CHANGE DETECTION

The spectral band ratio is one of the most common mathematical operations applied to multi-spectral data. Image ratios were calculated as the divisions of digital number values (0–255) in one spectral band by the corresponding pixel value in another band. After pre-processing of downloaded band 3 and band 4 images, the *NDVI* range was determined at 0.06 to 0.64.

NDVI values calculated for the 1986 indicated that values for many areas ranged from 0.40-0.60. This showed that at that time the vegetation was quite healthy and of high forest cover. The middle and other parts of the study area marked red had low *NDVI* values ranging from 0.06–0.26. It indicated that the area had a poor vegetation cover. The final image output of 1986 *NDVI* is shown in Figure 8a.

The raster calculation of the *NDVI* value was based on band 3 and 4 images. Using these values for 2010, the recognised minimum, maximum and mean *NDVI* values were 0.00, 0.77 and 0.59, respectively (Fig. 8b). These values indicated that on average the vegetation was healthier than that of 1986. Most areas and middle part of the area had low values reflecting poor vegetation performance.

In the case of *NDVI* values calculated for the 2016 forest cover, Landsat imagery show that *NDVI* values range between –0.075 and 0.12 (Fig. 8c). The result clearly indicated that in a large area vegetation was not healthy. It was clear that there was almost no healthy vegetation in the region. A very large area had *NDVI* values between –0.025 and 0.074, which classified the region as unhealthy. Moreover, a very small region, with *NDVI* values ranging from 0.10–0.12, would correspond to a relatively healthy vegetation cover.

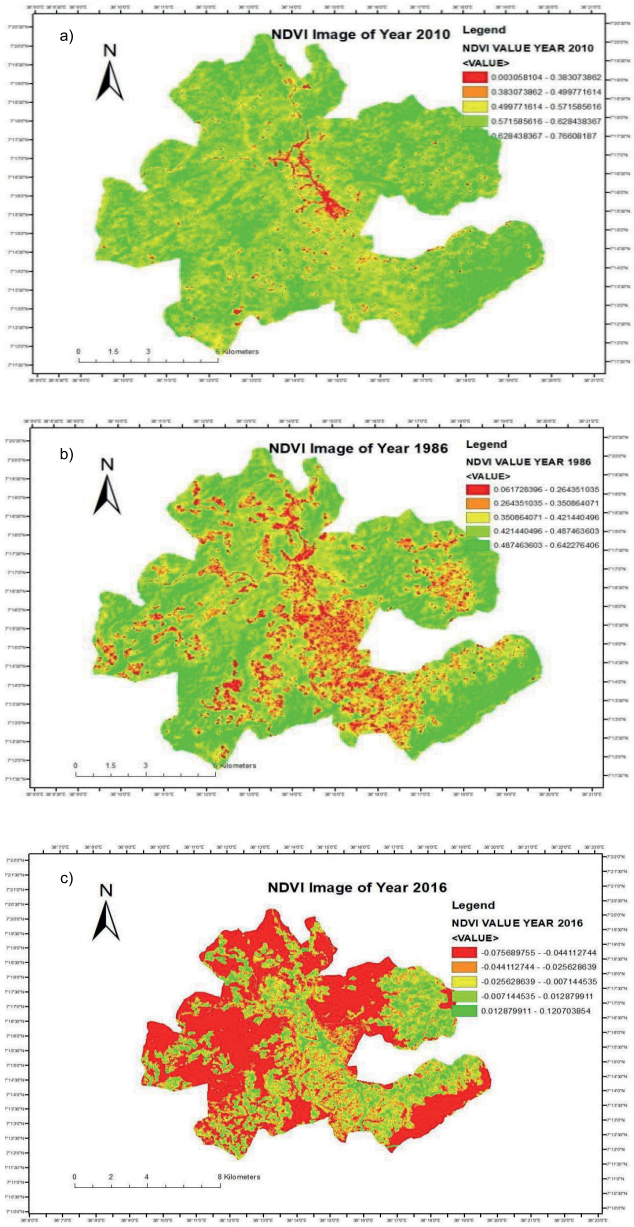

Fig. 8. Normalised difference vegetation index (*NDVI*) image of: a) 1986, b) 2010, c) 2016; source: own study

STASTICAL ANALYSIS OF *NDVI* FOR 1986, 2010 AND 2016 IMAGES

NDVI differences for particular images provide overall information about the health of the vegetation cover in the study area based on *NDVI* values. For this study, we used ETM+ (band 4 and band 3) to calculate *NDVI* values. The new version of ERDAS imaging software automatically calculates *NDVI* values. The negative threshold value indicates loss in the *NDVI* and a positive threshold value indicates areas of increased *NDVI*. In consecutive years, minimum, maximum and mean values fluctuated. It generally indicated that the overall vegetation was not in a stable condition. In 1986, the vegetation disturbance rate was higher than that of 2010. When we compared that to 2010 and 2018 image statistical values, the minimum value of 0.06 in 2010 decreased to 0 and the maximum value decreased from 0.77 to 0.12. It indicated that there was highly unprotected destruction of vegetation in 2016. In general, most part of the study area was relatively disturbed when compared to previous years.

RELATIONSHIP BETWEEN 1986 *NDVI* VALUES AND TEMPERATURE AND RAINFALL DATA

As *NDVI* increased, rainfalls become high and the temperature was low. The year of 1986 brought a lot of rainfall in the region and the temperatures were not high except for a small part of the region. In 2010, the area noted a lot of rainfall and temperatures were not high except for a small region in the area. The *NDVI* values indicated healthy vegetation which was brought about by the high rainfall and favourable temperatures. In 2016, the temperatures were high in most of the region. This indicated that majority of the study area was covered with unhealthy vegetation and rainfall experienced was minimal and caused vegetation to be unhealthy in most parts of the region (Fig. 9).

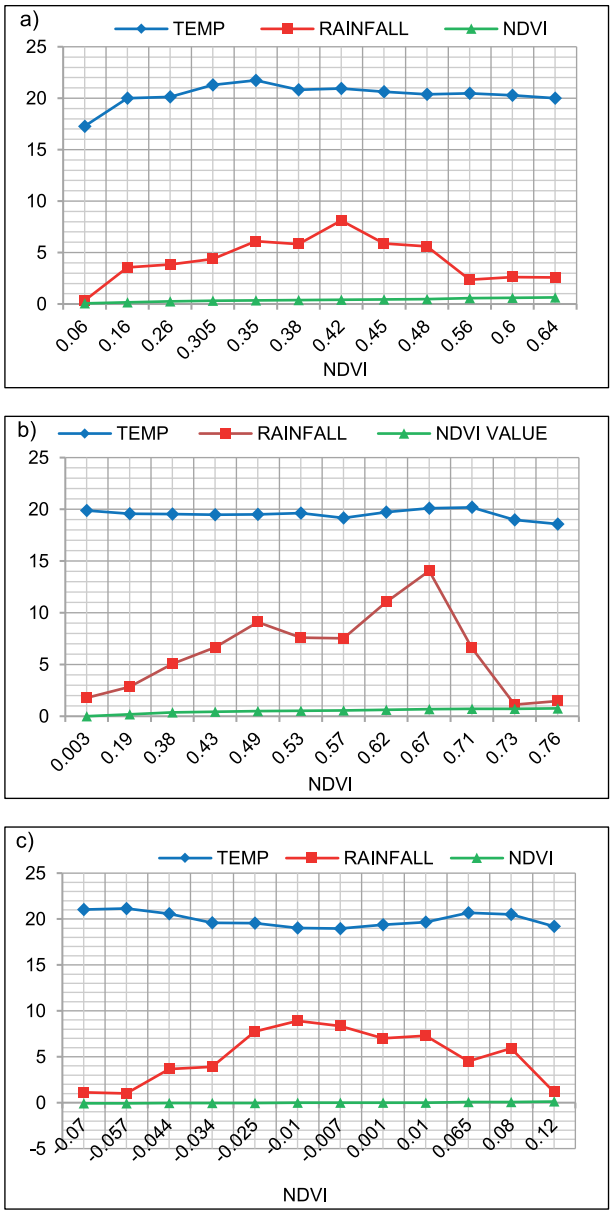

Fig. 9. Normalised difference vegetation index (*NDVI*), temperature and rainfall data for: a) 1986, b) 2010, c) 2016; source: own study

CONCLUSIONS

In this study, an attempt has been made to use geospatial techniques to detect spatial-temporal forest cover change in the Kafa zone using three sets of Landsat imagery. The results indicated that there was a clear change in the spatial extent of the forest cover within the 30 years period. Expansion of settlements and farmland resulted in the decline of both forest and wetland areas. The correlation between forest cover change and climate variability determined using ERDAS 9.2, ArcGIS v 10.4.1 and Pivot Table in Excel 2010 showed that the overall condition of forest cover change had ups and downs during the study period. Normalised difference vegetation index (*NDVI*) and net land cover change revealed that the forest cover changed from 10 020.33 ha to 8 851.23 ha, respectively between 1986 and 2018. The *NDVI* values between 0.06–0.64 in 1986 became 0.08 to 0.12 in 2018, which indicated a clear decline in forest cover within the 30 years period. The social, economic and environmental impacts of forest cover reduction should be studied in the future.

ACKNOWLEDGEMENTS

The authors gratefully acknowledge the ExiST project: Excellence in Science and Technology, Ethiopia, funded by KfW, Germany, through Jimma Institute of Technology, Center of Excellence, which covered the article processing charge.

REFERENCES

Al-Doski J., Mansor S., Shafri H. 2013. Change detection process and techniques. Civil and Environmental Research. Vol. 3(10) p. 37–46.

Alawamy J.S., Balasundram S.K., Hanif A.H.M., Sung C.T.B. 2020. Detecting and analyzing land use and land cover changes in the Region of Al-Jabal Al-Akhdar, Libya using time-series landsat data from 1985 to 2017. Sustainability (Switzerland). Vol. 12(11). DOI 10.3390/su12114490.

Alqurashi A.F., Kumar L. 2014. Land use and land cover change detection in the Saudi Arabian desert cities of Makkah and Al-Taif using satellite data. Advances in Remote Sensing. Vol. 3(3) p. 106–119. DOI 10.4236/ars.2014.33009.

Appiah D.O., Schröder D., Forkuo E.K., Bugri J.T. 2015. Application of geo-information techniques in land use and land cover change analysis in a peri-urban district of Ghana. ISPRS International Journal of Geo-Information. Vol. 4(3) p. 1265–1289. DOI 10.3390/ijgi4031265

Attri P., Chaudhry S., Sharma S. 2015. Remote sensing & GIS based approaches for LULC change detection – A review. International Journal of Current Engineering and Technology. Vol. 5(5) p. 3126–3137.

Austrian MAB Committee 2011. Biosphere reserves in the mountains of the world. Excellence in the clouds? Vienna. Austrian Academy of Sciences Press pp. 120.

Ayele G., Hayicho H., Alemu M. 2019. Land use land cover change detection and deforestation modeling: In Delomena District of Bale Zone, Ethiopia. Journal of Environmental Protection. Vol. 10(04) p. 532–561. DOI 10.4236/jep.2019.104031.

Bender S., Tekle M. undated. Community action for biodiversity and forest conservation and adaptation to climate change in the wild coffee forests (CAFA). Springer International Publishing.

Cheng S., Hiwatashi Y., Imai H., Naito M., Numata T. 1998. Deforestation and degradation of natural resources in Ethiopia: Forest management implications from a case study in the Belete-Gera Forest. Journal of Forest Research. Vol. 3(4) p. 199–204. DOI 10.1007/bf02762193.

Coppin P., Jonckheere I., Nackaerts K., Muys B., Lambin E. 2004. Digital change detection methods in ecosystem monitoring: A review. International Journal of Remote Sensing. Vol. 25(9) p. 1565–1596. DOI 10.1080/0143116031000101675.

Coppin P.R., Bauer M.E. 1996. Digital change detection in forest ecosystems with remote sensing imagery. Remote Sensing Reviews. Vol. 13(3–4) p. 207–234. DOI 10.1080/02757259609532305.

Danano K.A., Legesse A., Likisa D. 2018. Monitoring deforestation in South Western Ethiopia using geospatial technologies. Journal of Remote Sensing & GIS. Vol. 07(01) p. 1–5. DOI 10.4172/2469-4134.1000229.

Dong Y., Forster B., Ticehurst C. 1997. Radar backscatter analysis for urban environments. International Journal of Remote Sensing. Vol. 18(6) p. 1351–1364. DOI 10.1080/014311697218467.

Engdawork A., Bork H. 2014. Long-term indigenous soil conservation technology in the Chencha Area, Southern Ethiopia: Origin, Characteristics, and Sustainability. AMBIO. Vol. 43 p. 932–942. DOI 10.1007/s13280-014-0527-6.

Ferreira A.F., Zimmermann H., Santos R., von Wehrden H. 2020. Biosphere reserves' management effectiveness – A systematic literature review and a research agenda. Sustainability (Switzerland). Vol. 12(12) p. 1–31. DOI 10.3390/SU12145497.

Fichera C.R., Modica G., Pollino M. 2012. Land cover classification and change-detection analysis using multi-temporal remote sensed imagery and landscape metrics. European Journal of Remote Sensing. Vol. 45(1) p. 1–18. DOI 10.5721/EuJRS20124501.

Gandhi G.M., Parthiban S., Thummalu N., Christy A. 2015. NDVI: Vegetation change detection using remote sensing and Gis – A case study of Vellore District. Procedia Computer Science. Vol. 57 p. 1199–1210. DOI 10.1016/j.procs.2015.07.415.

Gebru T.D. 2016. Deforestation in Ethiopia: causes, impacts and remedy. International Journal of Engineering Development and Research. Vol. 4(2) p. 2321–9939.

Hassan Z., Shabbir R., Ahmad S.S., Malik A.H., Aziz N., Butt A., Erum S. 2016. Dynamics of land use and land cover change (LULCC) using geospatial techniques: a case study of Islamabad Pakistan. Springer Plus. Vol. 5(1). DOI 10.1186/s40064-016-2414-z.

Huete A., Didan K., Miura T., Rodriguez E.P., Gao X., Ferreira L.G. 2002. Overview of the radiometric and biophysical performance of the MODIS vegetation indices. Remote Sensing of Environment. Vol. 83(1–2) p. 195–213. DOI 10.1016/S0034-4257(02)00096-2.

Maina J., Wandiga S., Gyampoh B., Charles K.K.G. 2020. Assessment of land use and land cover change using GIS and remote sensing: A case study of Kieni, Central Kenya. Journal of Remote Sensing & GIS. Vol. 09(01) p. 1–5. DOI 10.35248/2469-4134.20.9.270.

Kennedy R.E., Townsend P.A., Gross J.E., Cohen W.B., Bolstad P., Wang Y.Q., Adams P. 2009. Remote sensing change detection tools for natural resource managers: Understanding concepts and tradeoffs in the design of landscape monitoring projects. Remote Sensing of Environment. Vol. 113(7) p. 1382–1396. DOI 10.1016/j.rse.2008.07.018.

Kogo B.K., Kumar L., Koech R. 2019. Forest cover dynamics and underlying driving forces affecting ecosystem services in western Kenya. Remote Sensing Applications: Society and Environment. Vol. 14 p. 75–83. DOI 10.1016/j.rsase.2019.02.007.

Lu D., Mausel P., Brondízio E., Moran E. 2016. Change detection techniques. International Journal of Remote Sensing. Vol. 25 p. 2365–2401. DOI 10.1080/0143116031000139863.

Mancino G., Nolè A., Ripullone F., Ferrara A. 2014. Landsat TM imagery and NDVI differencing to detect vegetation change: Assessing natural forest expansion in Basilicata, southern Italy. iForest – Biogeosciences and Forestry. Vol. 7(2) p. 75–84. DOI 10.3832/ifor0909-007.

NABU 2017. NABU's biodiversity assessment at the Kafa Biosphere Reserve [online]. Berlin, Addis Ababa. The Nature and Biodiversity Conservation Union. ISBN 978-3-925815-30-0 pp. 355. [Access 20.07.2020]. Available at: http://imperia.verbandsnetz.nabu.de/imperia/md/content/nabude/international/nabu_biodiversity_assessment_15.pdf

Negassa M.D., Mallie D.T., Gemeda D.O. 2020. Forest cover change detection using Geographic Information Systems and remote sensing techniques: a spatio-temporal study on Komto protected forest priority area, East Wollega Zone, Ethiopia. Environmental Systems Research. Vol. 9(1) p. 1–14. DOI 10.1186/s40068-020-0163-z.

Oljirra A. 2019. The causes, consequences and remedies of deforestation in Ethiopia. Journal of Degraded and Mining Lands Management. Vol. 6(3) p. 1747–1754. DOI 10.15243/jdmlm.2019.063.1747.

Othow O.O., Legesse Gebre S., Obsi Gemeda D. 2017. Analyzing the rate of land use and land cover change and determining the causes of forest cover change in Gog District, Gambella Regional State, Ethiopia. Journal of Remote Sensing & GIS. Vol. 06(04). DOI 10.4172/2469-4134.1000219.

Pongratz J., Caldeira K. 2012. Attribution of atmospheric CO_2 and temperature increases to regions: Importance of preindustrial land use change. Environmental Research Letters. Vol. 7(3). DOI 10.1088/1748-9326/7/3/034001.

Singh A. 1989. Review article digital change detection techniques using remotely-sensed data. International Journal of Remote Sensing. Vol. 10(6) p. 989–1003. DOI 10.1080/01431168908903939.

Stow D., Petersen A., Hope A., Engstrom R., Coulter L. 2007. Greenness trends of Arctic tundra vegetation in the 1990s: Comparison of two NDVI data sets from NOAA AVHRR systems. International Journal of Remote Sensing. Vol. 28(21) p. 4807–4822. DOI 10.1080/01431160701264284.

Tadesse G., Zavaleta E., Shennan C., FitzSimmons M. 2014. Policy and demographic factors shape deforestation patterns and socio-ecological processes in southwest Ethiopian coffee agroecosystems. Applied Geography. Vol. 54 p. 149–159. DOI 10.1016/j.apgeog.2014.08.001.

Verbesselt J., Zeileis A., Herold M. 2012. Near real-time disturbance detection using satellite image time series. Remote Sensing of Environment. Vol. 123 p. 98–108. DOI 10.1016/j.rse.2012.02.022.

Wang S.W., Gebru B.M., Lamchin M., Kayastha R.B., Lee W.K. 2020. Land use and land cover change detection and prediction in the Kathmandu district of Nepal using remote sensing and GIS. Sustainability (Switzerland). Vol. 12(9). DOI 10.3390/su12093925.

Weng Q. 2001. A remote sensing? GIS evaluation of urban expansion and its impact on surface temperature in the Zhujiang Delta, China. International Journal of Remote Sensing. Vol. 22(10) p. 1999–2014. DOI 10.1080/713860788.

Xiuwan C. 2002. Using remote sensing and GIS to analyse land cover change and its impacts on regional sustainable development. International Journal of Remote Sensing. Vol. 23(1) p. 107–124. DOI 10.1080/01431160010007051.

Yismaw A. 2014. Forest cover change detection using remote sensing and GIS in Banja District, Amhara Region, Ethiopia. International Journal of Environmental Monitoring and Analysis. Vol. 2 (6) p. 354. DOI 10.11648/j.ijema.20140206.19.

Zawadzki J., Cieszewski C.J., Zasada M., Lowe R.C. 2005. Applying geostatistics for investigations of forest ecosystems using remote sensing imagery. Silva Fennica Monographs. Vol. 39(4) p. 599–617. DOI 10.14214/sf.369.

Zhu Z., Woodcock C.E. 2014. Continuous change detection and classification of land cover using all available Landsat data. Remote Sensing of Environment. Vol. 144 p. 152–171. DOI 10.1016/j.rse.2014.01.011.

Ziboon A.R., Imzahim I., Khalaf A.G. 2013. Utilization of remote sensing data and GIS applications for determination of the land cover change in Karbala Governorate. Vol. 31(15) p. 2773–2787.